Krzysztof Baszczyński

Modeling the Performance of Horizontal Anchor Lines during Fall Arrest

DOI: 10.5604/01.3001.0010.4634

Central Institute for Labour Protection
– National Research Institute,
Department of Personal Protective Equipment,
Wierzbowa 48, 90-133 Łódź
E-mail: krbas@ciop.lodz.p

Abstract
The basic materials used for the construction of anchor lines for personal equipment protection against falls from a height are ropes and textile webbing. During fall arrest, horizontal anchor lines significantly affect the forces acting on the worker and the work site elements, as well as the fall arrest distance. Manufacturers of the equipment are required to estimate those parameters for various conditions of use by numerical simulations with a validated model. The model discussed in this paper reflects the mechanical structure of the line (whether singles-span or multi-span) taking into account Maxwell's and Kelvin–Voigt's non-linear rheological models for viscoelastic materials. The model consists of a system of seven non-linear differential equations with the parameters describing static load-elongation characteristics and time-courses of dynamic loading forces for selected ropes and textile webbing. The numerical model developed was used to simulate the performance of horizontal anchor lines of different constructions. The model was validated by comparing the numerical calculations with laboratory test results and was shown to be sufficiently accurate to be used for designing fall protection equipment.

Key words: *protective equipment, falls from a height, horizontal anchor lines, webbing, fibre rope, elongation, performance test.*

Introduction

On many elevated work sites, e.g., in the construction, mining, and energy industries, workers must be able to move horizontally to perform their tasks. Examples of such work sites and tasks include renovation of walls and roofs, the erection and maintenance of steel structures, the servicing of industrial installations, etc. Workers carrying out such activity should be protected against falls in a way that would not compromise their comfort. If collective protection measures cannot be implemented for technical or economic reasons, then one should consider the use of individual fall protection systems. Given existing knowledge [1-3] and relevant OSH regulations [4-6], in the case of temporary works the best solution is to deploy a protection system consisting of the following:

- a horizontal anchor line,
- a connecting and shock-absorbing assembly (e.g., lanyard with an energy absorber, self-locking arrester on a flexible line),
- a full body harness.

Figure 1 shows an example of a fall protection system incorporating a horizontal anchor line.

If the worker needs to move horizontally up to a distance of several meters, the anchor line is usually attached only to two extremity anchor points (2) in a single-span system. In the case of longer distances, intermediate anchor points are used (3) to enable a greater range of movement while still ensuring fall protection. Among the above-mentioned elements, of particular note is the horizontal anchor line because during fall arrest it exerts a significant influence on:

- the fall arrest distance,
- the force acting on the human body through the safety harness,
- the force acting on elements of the work site through the anchor points.

Examples of anchor lines are given in ***Figure 2*** (see page 96).

The parameters discussed above have a direct effect on user safety. For this reason, according to the requirements of standard EN 795:2012 [5] and directive 89/686/EEC [7], the determination of the maximum deflection of the anchor line and the forces acting in it is the condition for starting the use of the equipment. This problem is solved in laboratories by conducting an assessment of the equipment and preparing new constructions.

Miura and Sulowski [8] presented a comprehensive work on the mechanical factors involved in the performance of horizontal anchor lines. They used catenary methods

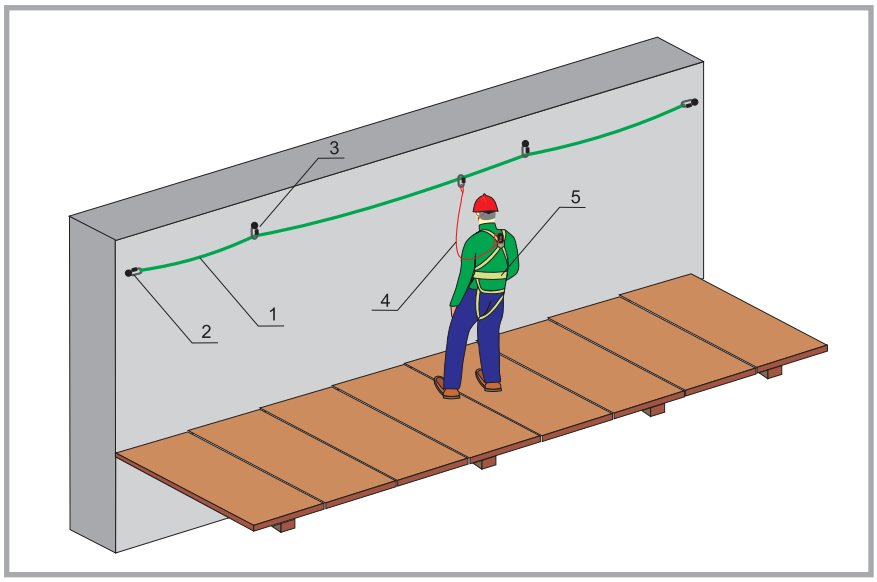

Figure 1. *Fall protection system enabling workers to move horizontally: 1 – horizontal anchor line, 2 – extremity anchor point, 3 – intermediate anchor point, 4 – lanyard, 5 – full body harness.*

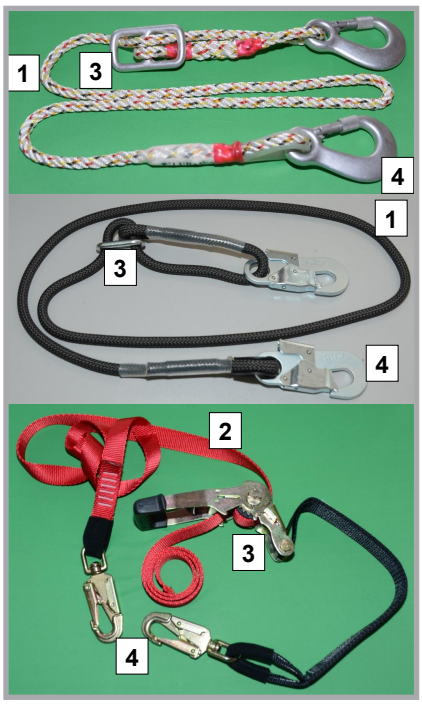

Figure 2. *Examples of horizontal anchor lines: 1 – textile rope, 2 – textile webbing, 3 – tensioner, 4 – connector.*

as well as potential energy–strain energy analysis to describe the performance of textile and steel horizontal lines during fall arrest and to determine the maximum deflection and forces in the lines. Publication [9] examined the performance of textile horizontal anchor lines, analysing the non-linear load-elongation characteristics of a three-strand twisted polyamide rope with a diameter of 14 mm. The model presented in [9] was simplified in that it assumed the characteristics of textile ropes to be independent of elongation velocity. The paper also presented an experimental stand for dynamic testing of horizontal anchor lines and compared the results of laboratory tests with computer simulations carried out pursuant to the model developed. The construction and use of horizontal anchor lines made of textile and steel ropes was also addressed in publications [1, 3]. In addition, those papers discussed the requirements imposed on such lines and problems concerning their installation on work sites.

The mechanical characteristics of textile materials, such as ropes and webbing, used in fall protection equipment were examined in publications [10, 11], which focused on load-elongation characteristics, with the test results obtained being applied in numerical models simulating the performance of connecting and shock-absorbing assemblies during fall arrest. The models and characteristics presented in those papers were used in the development of the horizontal anchor line model presented herein. The dynamic loading of lanyard webbing used in fall protection equipment was investigated in a British study reported in a Health and Safety Laboratory (HSL) publication [12]. The most important issue analysed in that report was the effect of loading velocity on the breaking strength of textile webbing. Bedogni and Manes [13] modeled the dynamic performance of mountaineering ropes under repetitive loading during fall arrest. The influence of multiple loading of textile ropes and webbing on their load-elongation characteristics was discussed by Baszczyński [14]. The development and identification of a variety of models (including rheological ones) for textile structures was presented in publications [15-21].

Due to the significance of the problem and previous results, the Central Institute for Labour Protection – National Research Institute undertook efforts to develop a new numerical model of the performance of textile horizontal anchor lines during fall arrest. The model was originally designed for conducting numerical simulations of the performance of single and multi-span anchor lines with different construction parameters, made of different textile materials, and subjected to a range of dynamic forces. The nonlinearity of the load-elongation characteristics of textile ropes and webbing and their dependence on the elongation velocity were two of the most important assumptions for the model. It was also assumed that the model should allow to simulate the time courses of the most important mechanical quantities characterising the performance of horizontal anchor lines.

This paper discusses the results of those efforts, that is, the numerical model developed, simulations of single-span and three-span anchor lines, and validation of the model through laboratory testing.

Simulation and study materials

Reusable horizontal anchor lines commercially available in Europe are made of a variety of textile materials. In terms of construction, most of them are fabricated from twisted or woven ropes with or without cores, or from polyamide, polyester, or aramid webbing. Therefore for the purposes of horizontal anchor line modeling, some of those typical materials which behave differently under dynamic conditions (during fall arrest) were selected based on the characteristics of textile ropes and webbing provided in papers [10, 11]. The materials studied are described in ***Table 1***.

The materials were used to make anchor lines for laboratory tests validating the models developed. The anchor lines were 2.5 m to 15 m long and terminated in loops for attachment to the fall arrest experimental stand. Depending on the material, the loops were sewn or spliced. A typical connector made from a 10 mm diameter metal bar was put through each loop.

Horizontal anchor line model

A horizontal anchor line model was developed for the system presented in ***Figure 3***.

The following assumptions were adopted for the purposes of determining the structure and parameters of the horizontal anchor line model [15-21]:

- the model describes the movement of a rigid test mass whose fall is arrested by a horizontal anchor line, from the end of the free fall phase to the point when the maximum elongation is reached (the test mass is in the lowest position);
- the basic parameters describing the fall arrest process are as follows: the test mass displacement, fall arrest force, and the force acting on the points in which the line is anchored to fixed work site elements;

Table 1. *Textile materials used in simulations and for preparation of anchor lines tested.*

Symbol	Material and construction	Designation (manufacturer)
A	Three-strand polyamide fibre rope, 12 mm in diameter	PA 12-A-Z/KG/200 (Bezalin S.A., Poland)
B	Core rope, 12 mm in diameter, aramid core with polyamide mantle	LB 201 FLR (Protekt – Grzegorz Łaszkiewicz, Poland)
C	Polyamide webbing, 45 mm wide	L1 TS 325/45 (PASAMON" Sp. z o.o., Poland)

- the test mass is perfectly rigid and its dimensions are ignored;
- the extremity and intermediate anchor points are perfectly rigid;
- the anchor line slides through the intermediate anchor points without friction;
- the model describes single- and three-span horizontal anchor lines;
- the anchor line is loaded halfway between the extremity or intermediate anchor points;
- at the beginning of the fall, the angle between the anchor line and the imaginary horizontal plane is 0°, with the initial tension being negligibly small;
- the rigid test mass is connected to the anchor line by means of an inextensible lanyard of negligible weight;
- the model takes into account the non-linear load-elongation characteristics of textile ropes and webbing [10], and it is assumed that those characteristics change with the elongation velocity;
- the input variables are as follows: m – weight of the test mass, h – free fall distance of the test mass, load-elongation characteristics of the textile material, L_0 – span length for the single-span version (or L_0 and L_b for the multi-span version),
- the model does not take into account the phenomena occurring within the rope or webbing.

In the first step of model development, the movement of a rigid test mass during fall arrest (as shown in ***Figure 3***) is described by means of the following ***Equations (1), (2)***:

$$m \cdot \frac{d^2x}{dt^2} = Q - F_x \tag{1}$$

$$Q = m \cdot g \tag{2}$$

where:
x – vertical displacement of the rigid test mass,
m – weight of the rigid test mass,
Q – force of gravity acting on the test mass,
g – gravitational acceleration,
F_x – fall arrest force generated by the elongation of the anchor line.

From the geometric relationships given in ***Figure 4***, it follows that:

$$\left(\frac{L_0}{2}\right)^2 + x^2 = y^2 \tag{3}$$

$$\frac{x}{y} = \frac{F_x}{2F_y} \tag{4}$$

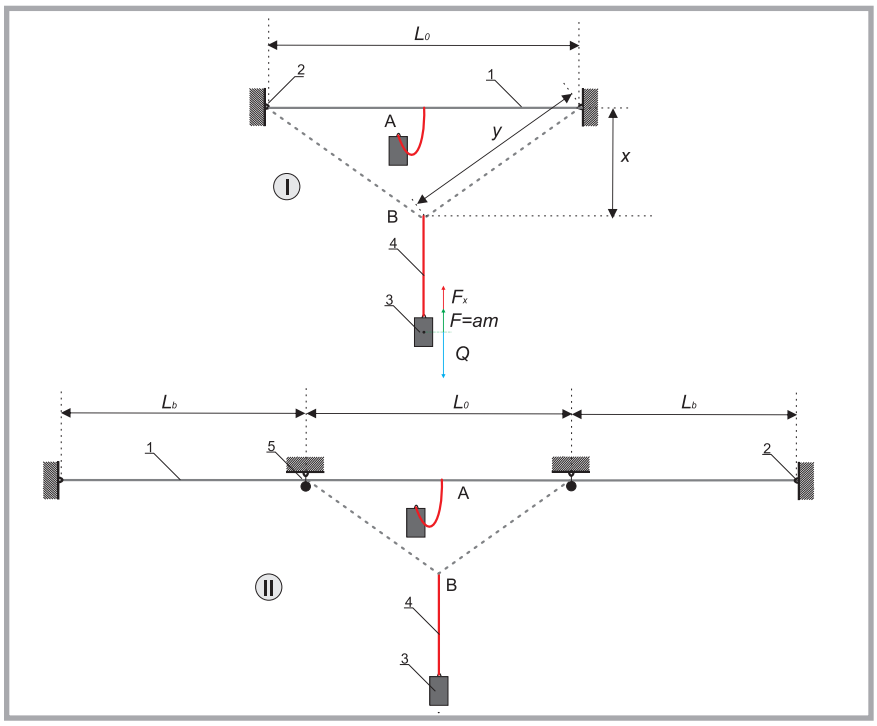

Figure 3. *Scheme of loading a horizontal anchor line: I – single-span anchor line, II – three-span anchor line, A – test mass position at the beginning of the fall, B – test mass position after the fall arrest, 1 – rope/webbing, 2 – extremity anchor point, 3 – rigid test mass, 4 – inextensible lanyard, 5 – intermediate anchor point.*

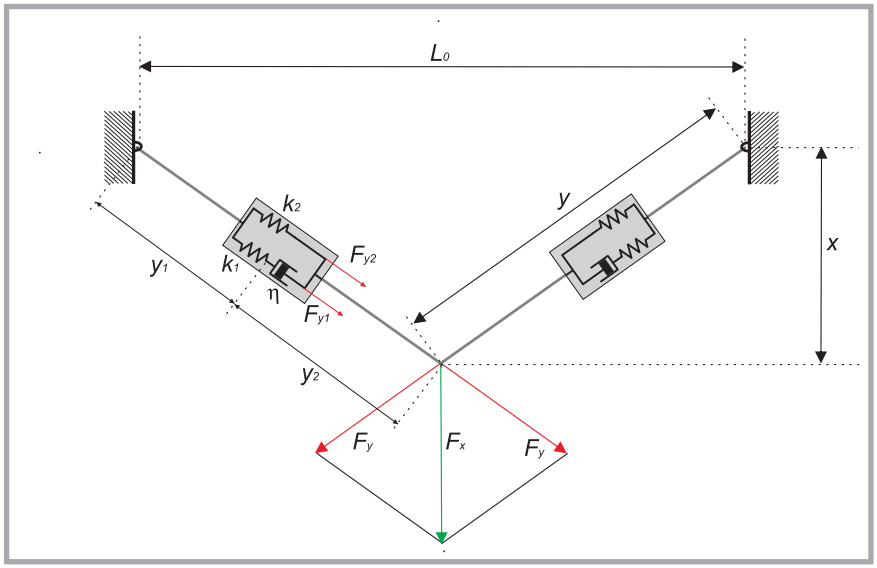

Figure 4. *Horizontal anchor line model: k_1 – elastic element with linear characteristics, k_2 – elastic element with non-linear characteristics, η – perfectly viscous element.*

and thus the movement ***Equation (5)*** for the test mass takes the form of:

$$m \cdot \frac{d^2x}{dt^2} + \frac{2 \cdot x \cdot F_y}{\sqrt{\left(\frac{L_0}{2}\right)^2 + x^2}} - Q = 0 \tag{5}$$

This equation involves the force F_y acting in the anchor line, which depends on the load-elongation characteristics of the textile material. To calculate that force, the model describing textile elements proposed in papers [11, 20, 21] was adopted. It is schematically presented in ***Figure 4***.

The model is based on the assumptions formulated above, as well as on Maxwell's, Kelvin–Voigt's and Zener's rheological models of viscoelastic elements [10, 13, 19-21]. In the model proposed,

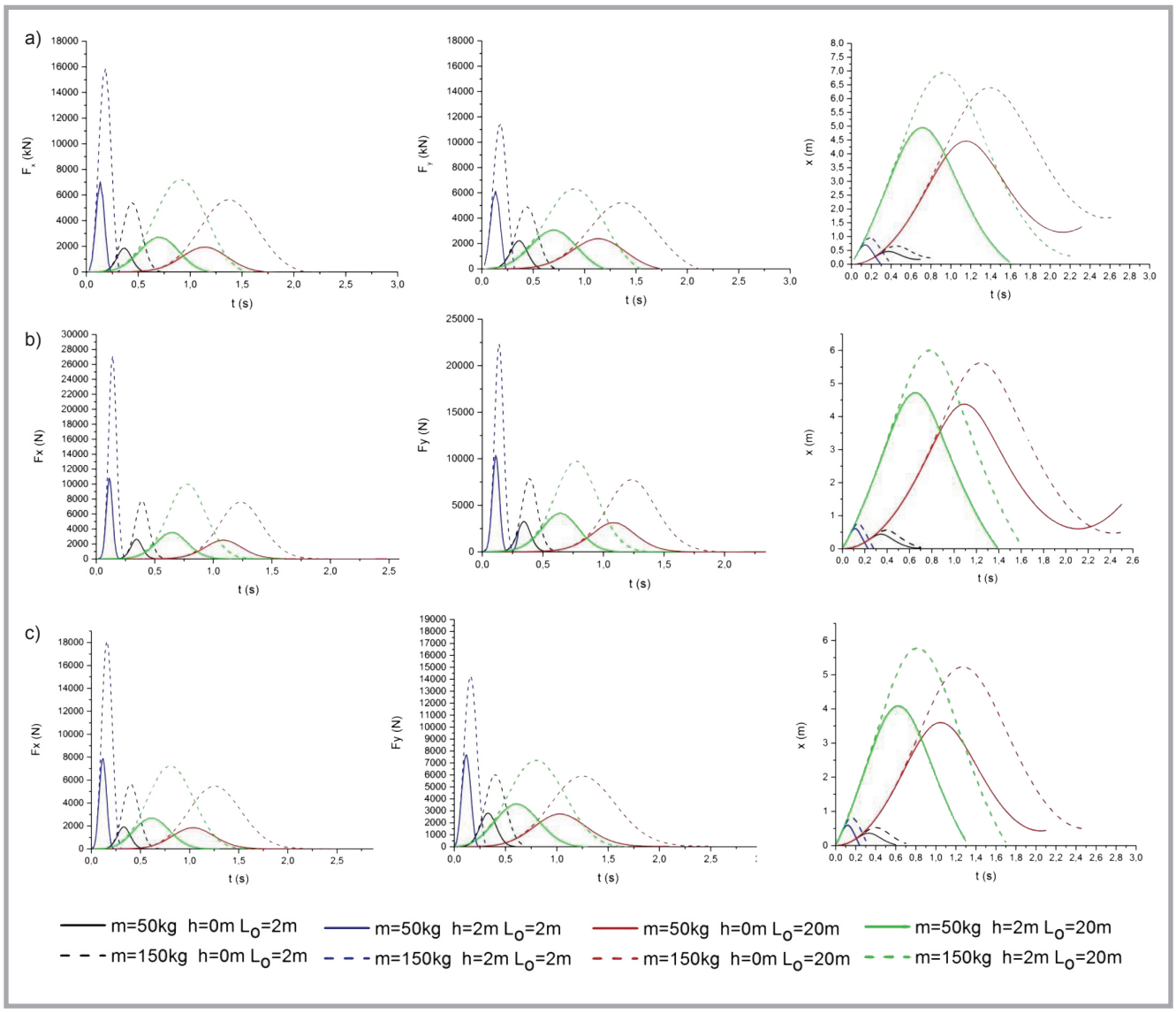

Figure 5. *Time courses of $F_x(t)$, $F_y(t)$, and $x(t)$ obtained by numerical simulation of the performance of a single-span horizontal anchor line.*

element k_2 with non-linear characteristics predominantly determines the behaviour under static loading, while elements k_1 and η predominantly determine that under dynamic loading.

Based on conclusions from paper [12], elements of the model given in ***Figure 5*** are described with the following ***Equations (6)***, ***(7)*** and ***(8)***

- elastic element k_2

$$F_{y2} = \left(b_0 \cdot \frac{L_{REF}}{\frac{L_0}{2}}\right)^{b_1} \cdot y^{b1} \qquad (6)$$

where:
$L_0/2$ – half of the length of the non-loaded anchor line,
L_{REF} – length of the non-loaded rope/webbing sample used in static tests,
b_0, b_1 – coefficients of the power function describing the $F_{y2}(y)$ characteristic,
y – elongation of element k_2,
F_{y2} – tensile force.

- elastic element k_1

$$F_{y1} = \frac{1}{\frac{L_0}{2 \cdot L_{REF}} \cdot k_1} \cdot y_1 \qquad (7)$$

where:
k_1 – linear characteristic slope coefficient,
y_1 – elongation of element k_1.

- perfectly viscous element η

$$F_{y1} = \frac{\eta}{\frac{L_0}{2 \cdot L_{REF}}} V \qquad (8)$$

where:
η – viscosity coefficient,
V – elongation velocity for element η.

An overall horizontal anchor line model was developed and expressed by the following system of equations describing the movement of a rigid test mass with a weight of m during fall arrest:

$$\begin{cases} m \cdot \frac{d^2x}{dt^2} + \frac{2 \cdot x \cdot F_y}{\sqrt{\left(\frac{L_0}{2}\right)^2 + x^2}} - Q = 0 \\ F_y = F_{y1} + F_{y2} \\ y = y_1 + y_2 \\ y_1 = \frac{L_0}{2 \cdot L_{REF}} k_1 F_{y1} \\ F_{y1} = \frac{\eta}{\frac{L_0}{2 \cdot L_{REF}}} \frac{dy_2}{dt} \\ F_{y2} = \left(b_0 \frac{2 \cdot L_{REF}}{L_0}\right)^{b_1} y^{b1} \end{cases} \qquad (9)$$

The system of ***Equations (9)*** proposed was solved using the Adams method and Backward Differentiation Formula method (BDF) in a program developed by means of Mathcad software (PTC, USA) [22], adopting the following initial conditions (for $t = 0$):

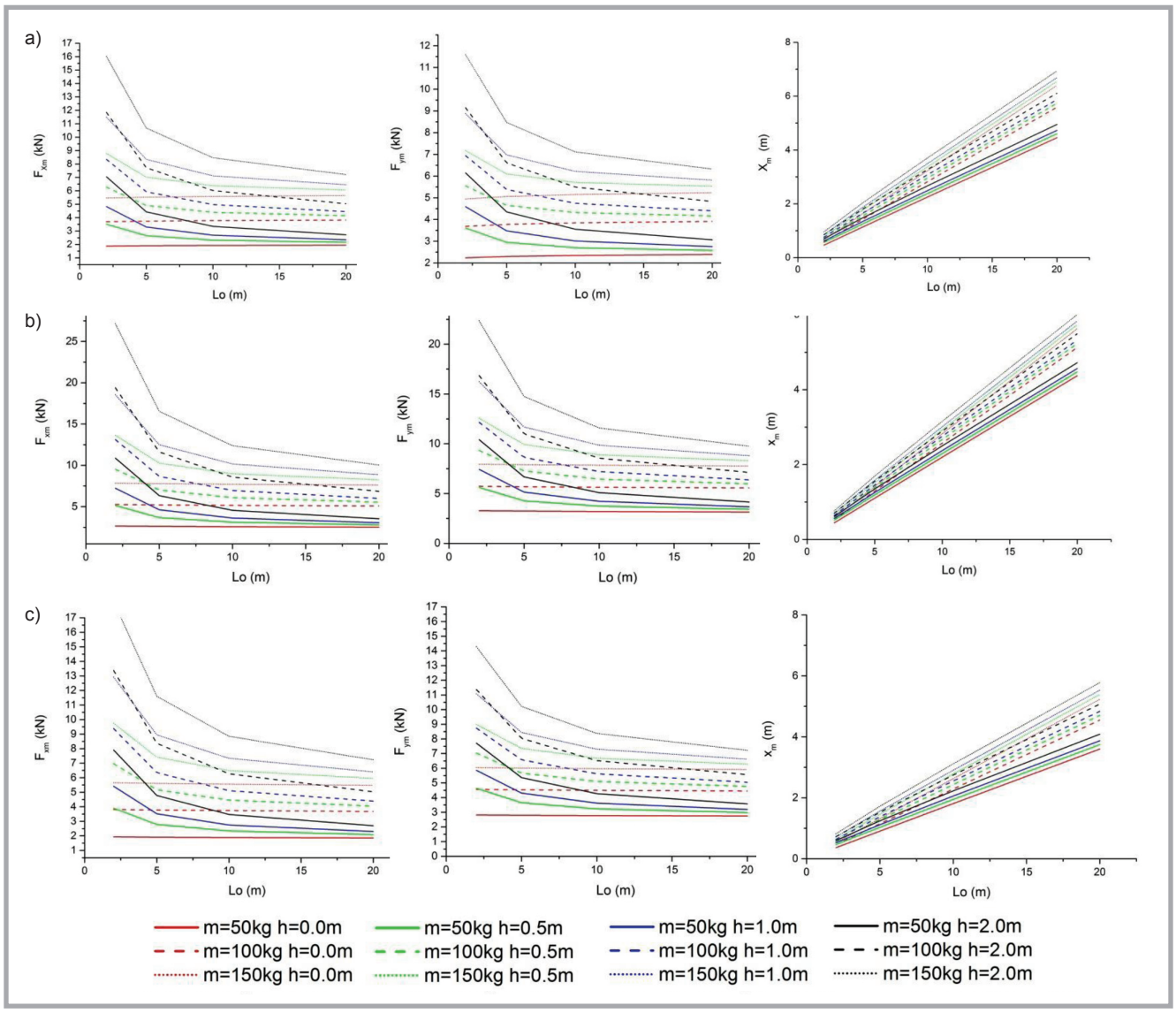

Figure 6. *Maximum values of F_{xm}, F_{ym}, and x_m obtained by numerical simulation of the performance of a single-span horizontal anchor line.*

- x*(0)* = 0 – initial displacement of the test mass,
- *V(0)* – velocity of the test mass at the beginning of fall arrest, calculated from:

$$V(0) = \sqrt{2hg} \qquad (10)$$

where:
h – distance travelled by the free-falling test mass

- *a(0)* = *g* – acceleration of the test mass at the beginning of fall arrest.

To fully define the model, it was necessary to specify the values of parameters b_0, b_1, η, and k_1 used in formulas (6) and (7), which describe the characteristics of the textile materials applied. Those values were taken from paper [11], which reported the characteristics of textile materials used in personal fall protection equipment as determined by laboratory testing of load-elongation characteristics and by the identification of characteristic parameters. The parameter values adopted are given in ***Table 2***.

Numerical simulations

The horizontal anchor line model developed was used in numerical simulations of mechanical phenomena accompanying fall arrest. The input variables included:

- L_o – distance between anchor points (span length for single-span anchor lines),
- L_o and L_c – distance between the extremity and intermediate anchor points, where $L_c = 2 \cdot L_b + L_o$ (for three-span anchor lines according to ***Figure 3***),
- *m* – weight of the rigid test mass,
- *h* – distance travelled by the free-falling test mass,
- b_0, b_1, η, k_1 coefficients characterising textile ropes/webbing designated as A, B, and C.

Table 2. *Specification of parameters b_0, b_1, k_1, and η.*

Symbol	L_{REF}, m	b_0	b_1	η	k_1
A	2.05	$1.295 \cdot 10^4$	1.259	$1.100 \cdot 10^3$	$1.902 \cdot 10^{-4}$
B	1.98	$1.581 \cdot 10^5$	1.610	$0.417 \cdot 10^3$	$1.666 \cdot 10^{-4}$
C	2.0	$2.537 \cdot 10^4$	1.074	$0.083 \cdot 10^3$	$1.990 \cdot 10^{-7}$

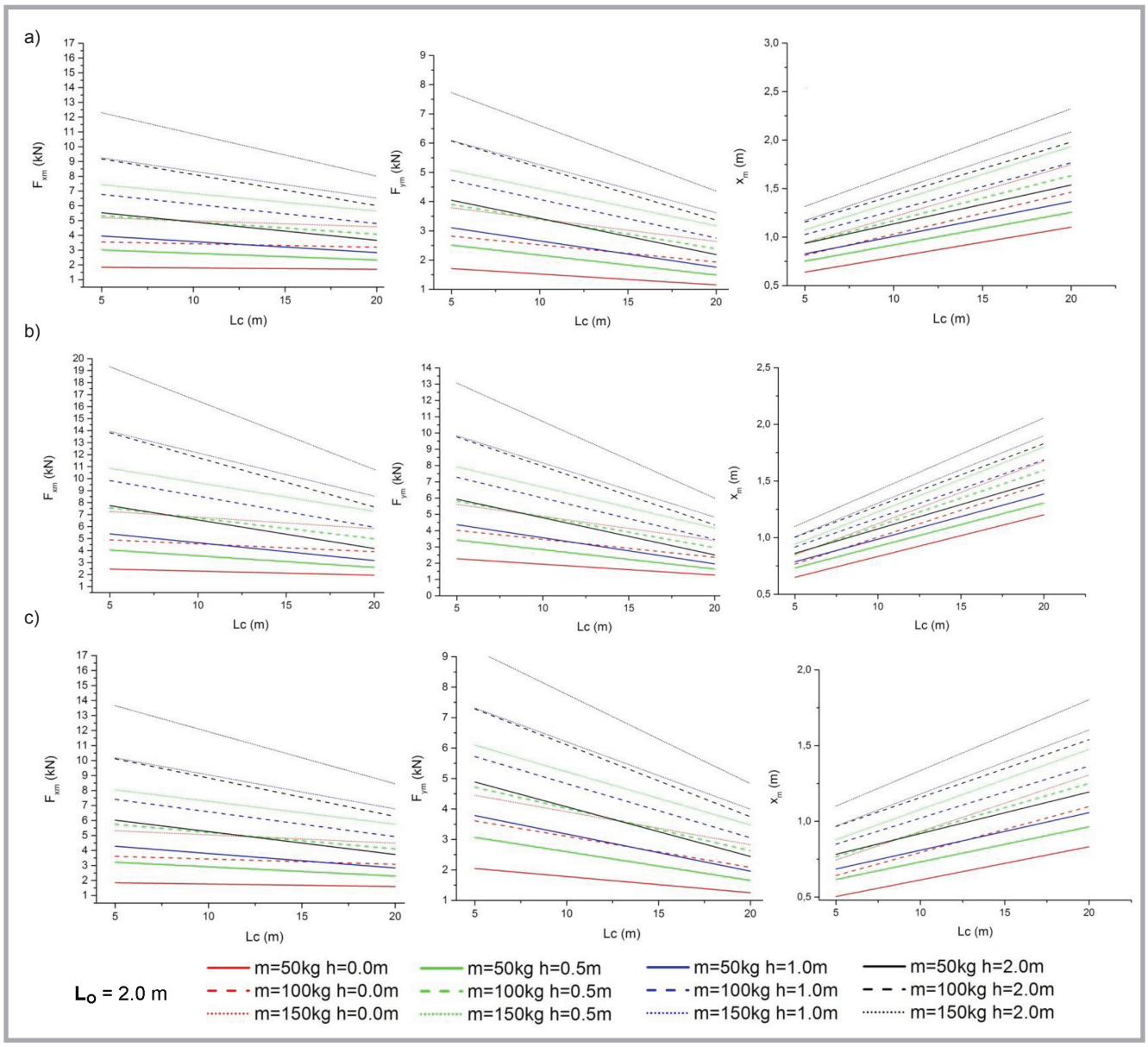

Figure 7. *Maximum values of F_{xm}, F_{ym}, and x_m obtained by numerical simulation of the performance of a three-span horizontal anchor line.*

The initial parameters characterising the performance of horizontal anchor lines were:

- F_x – fall arrest force,
- F_y – force acting on the extremity anchor points,
- x – deflection of the anchor line at the point of loading.

Simulation examples are given in ***Figures 5***, ***6*** and ***7***.

Analysis of the results obtained revealed the following:

- In the time courses of $F_x(t)$, $F_y(t)$, and $x(t)$, the time to peak (T_N) increased with the increasing weight of the test mass (m).
- In the time courses of $F_x(t)$, $F_y(t)$, and $x(t)$, the time to peak (T_N) was the shortest for rope B, followed by webbing C and rope A.
- In the time courses of $F_x(t)$, $F_y(t)$ and $x(t)$, the time to peak (T_N) increased with the increasing length of span L_o and decreased with the increasing distance travelled by the free-falling test mass (h).
- The highest maximum deflection x_m was found for rope A, followed by rope B and webbing C.
- The maximum deflection x_m increased with increasing parameters m, L_o & h.
- For $h > 0$ m, the longer the span L_o, the lower the fall arrest force F_{xm} and the lower the force F_{ym} acting on the extremity point. Forces F_{xm} and F_{ym} decreased most rapidly for $L_o < 10$ m.
- For $h = 0$ m, the fall arrest force F_{xm} was practically independent of the span length L_o.
- For low kinetic energy of the test mass ($m = 50$ kg and $h = 0$ m), the maximum forces acting on it were smaller than those acting on the anchor points F_{ym}.
- For $m > 50$ kg and $h > 0$ m, this relationship was reversed ($F_{xm} < F_{ym}$).
- For the same kinetic energy of the test mass, the highest values of F_{xm} and F_{ym} were found for rope B, followed by webbing C and rope A.
- A comparison of single-span and three-span anchor lines shows that for the same kinetic energy of the test mass, the maximum values of forces F_{xm} and F_{ym} were lower for the three-span line. The differences increased

with the increasing length of the side spans L_c.
- Higher deflection x_m was found for the three-span anchor line.

Validation of the model

The model developed was validated by comparing selected numerical simulations with the results of laboratory tests conducted on specially prepared horizontal anchor lines made of materials specified in ***Table 1***. The tests were carried out on the experimental stand presented in ***Figure 8***.

The tests measured three parameters:
- the arrest force exerted by the horizontal anchor line on the falling rigid test mass,
- the force acting on the extremity anchor points,
- the deflection of the anchor line at the point of loading.

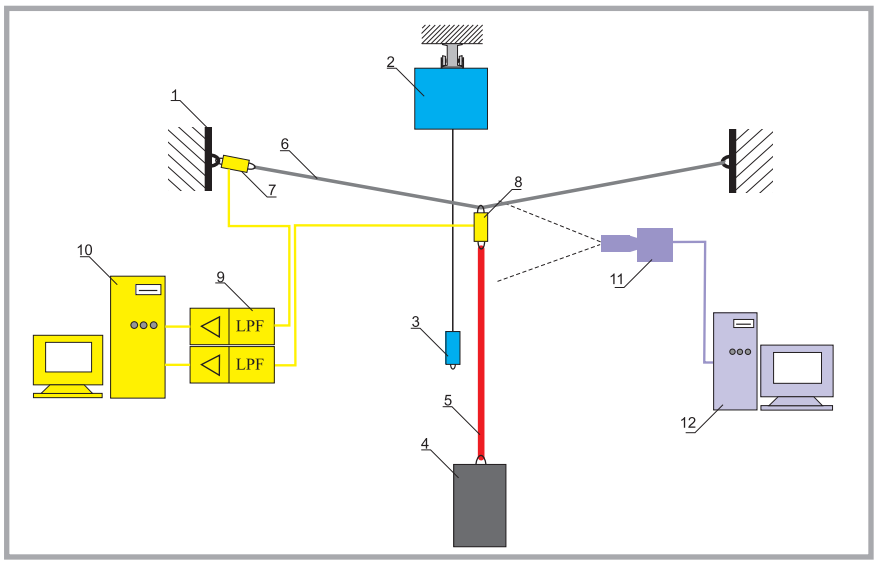

Figure 8. *Stand for testing flexible horizontal anchor lines under dynamic conditions: 1 – rigid frame, 2 – wall crane, 3 – electromagnetic latch, 4 – test mass of 100 kg, 5 – aramid lanyard, 6 – horizontal anchor line tested, 7, 8 – U9B-20kN force transducers (Hottinger, Germany), 9 – filters type MS210R (IMD, Germany) and analog amplifiers type AE-101 (Hottinger, Germany), 10 – KUSB 3116 type data acquisition system (DAS) (Keithley, USA), 11 – MotionBlitz EoSens Cube7 high speed digital camera (Mikrotron, Germany), 12 – computer coupled with the camera.*

For the purpose of measurements, the anchor line (6) was attached to anchors on the rigid frame meeting the requirements of standard EN 364:1996 [23] in terms of rigidity and resonance frequency. Loading was applied at the midpoint of the anchor line by means of a falling rigid test mass (4) weighing 100 kg. The test mass was connected to the anchor line tested using a 1.5 m long aramid lanyard (5) and force transducer (8). The lanyard (5) was characterised by significantly lower elongation as compared to the anchor line. The test mass was lifted, lowered and dropped by means of a wall crane (2) coupled with an electromagnetic latch (3). The force measurement apparatus consisted of force transducers type U9B-20kN (Hottinger, Germany) (7) and (8), amplifiers type AE-101 (Hottinger, Germany), low-pass analog filters type MS210R (IMD, Germany) of suitable characteristics (9), and the KUSB 3116 type data acquisition system (Keithley, USA) (10). The deflection of the horizontal anchor line, corresponding to the vertical displacement of the point at which the transducer (8) was connected to the anchor line, was recorded using the Mo-

Table 3. *Comparison of numerical simulations with the results of laboratory testing.*

Symbol of material	Simulation and test conditions			F_{xmt}	F_{xmp}	Δ_{Fx}	F_{ymt}	F_{ymp}	Δ_{Fy}	x_{mt}	x_{mp}	Δ_x
	m, kg	L_o, m	h, m	kN	kN	%	kN	kN	%	m	m	%
A	100	2.8	0.5	5.64	5.50	2.5	5.14	5.11	0.6	0.92	0.98	-6.5
		2.8	1.0	7.26	7.31	-0.7	6.25	6.93	-10.9	1.00	1.05	-5.0
		2.8	1.5	8.7	9.22	-6.0	7.20	7.80	-8.3	1.06	1.08	-1. 9
		2.8	2.0	10.02	10.7	-6.8	8.05	8.61	-7.0	1.12	1.12	0.0
		2.8	2.5	11.25	12.04	-7.0	8.82	9.83	-11.5	1.16	1.15	0. 9
		6.0	0.0	3.75	3.64	2.9	3.80	3.99	-5.1	1.71	1.79	-4.7
		6.0	0.5	4.74	5.05	-6.6	4.54	4.87	-7.2	1.84	1.96	-6.5
		6.0	1.0	5.64	5.93	-5.6	5.18	5.63	-8.7	1.94	2.04	-5.2
B		2.5	0.0	5.43	5.51	-1.5	7.66	7.43	3.0	0.47	0.50	-6.4
		2.5	1.0	14.40	15.26	-5.9	16.89	15.95	5.6	0.59	0.64	-8.5
		4.0	0.0	5,42	5.63	-3,9	7.65	6.99	-3.9	0.78	0.75	3,9
		4.0	1.0	11.34	12.08	-6.5	13.90	13.1	5.8	0.89	0.93	-4.5
		6.0	0.0	5.41	5.72	-5.73	7.632	7.24	5.14	1.14	1.09	4.4
		6.0	1.0	9.50	9.81	-3.3	12.05	11.52	4.4	1.29	1.18	8.5
C		2.5	0.0	3.81	3.40	10.7	4.55	4.30	5.5	0.58	0.51	12.0
		2.5	1.0	8.45	7.83	7.3	8.09	8.29	-2,5	0.77	0.72	6.5
		2.5	1.5	10.23	9.82	4,0	9.31	9.56	-2,7	0.82	0.75	8.5
		6.0	0.0	3.77	3.32	11.9	4.52	5.12	-13.2	1.37	1.21	11.6
		6.0	0.5	4.94	4.00	19,0	5.48	5.44	0.7	1.51	1.47	2.6
		6.0	1.0	5.95	5.12	13,9	6.27	6,40	-2.1	1.61	1.57	2.5
		6.0	1.5	6.86	6.10	11,1	6.96	7.12	-2.3	1.70	1.61	5.3

tionBlitz EoSens Cube7 high speed digital camera (Mikrotron, Germany) (11) coupled with a computer (12). The images recorded were analysed using specialized software – Tema Motion – Starter II (Image System, Sweden) [24].

The results of the tests carried out on the experimental stand described above are given in ***Table 3***, where:
F_{xmt} – maximum fall arrest force calculated,
F_{xmp} – maximum fall arrest force, measured
F_{ymt} – maximum force acting on the anchor points calculated,
F_{ymp} – maximum force acting on the anchor points measured,

$$\Delta_{Fx} = \frac{F_{xmt} - F_{xmp}}{F_{xmt}} \cdot 100 \qquad (11)$$

$$\Delta_{Fy} = \frac{F_{ymt} - F_{ymp}}{F_{ymt}} \cdot 100 \qquad (12)$$

$$\Delta_{x} = \frac{x_{mt} - x_{mp}}{x_{mt}} \cdot 100 \qquad (13)$$

Analysis of the results has revealed that:
- Differences between the values of F_{xm}, F_{ym} & x_m calculated and measured are acceptable as they do not exceed the 20% limit imposed by Standard PN-EN 795:2012 [5].
- The differences between simulation and measurement results observed are attributable both to imperfections of the model and to the uncertainty of measurement of the various mechanical parameters.

- The most important causes of discrepancies include:
  – energy absorption by the lanyard (5) (***Figure 8***) connecting the test weight to the anchor line,
  – initial deflection of the anchor line under the influence of gravity (prior to the fall of the test mass),
  – initial horizontal displacement of the test mass and the point of loading along the horizontal anchor line by approx. 200 mm caused by the construction of the experimental stand,
  – initial tensioning of the anchor line applied to reduce its deflection prior to dropping the test mass.

Conslusions

The validation tests conducted showed the numerical model of horizontal anchor lines presented to be sufficiently accurate to analyse the performance of such lines in fall arrest situations and to estimate the maximum values of the mechanical parameters relevant to human safety. The model and software developed may be used in conjunction with laboratory testing to obtain valuable information about the performance of different construction variants of horizontal anchor lines and their compatibility with other types of fall prevention equipment. The most important advantages of the model designed include:
- calculation of the time courses of parameters characterising the fall arrest process;
- calculation of the forces acting on the worker during fall arrest, enabling the selection of an appropriate connecting and shock-absorbing assembly, such as a textile shock-absorbing lanyard connecting the full body harness to the anchor line;
- calculation of the maximum deflection of the horizontal anchor line corresponding to the fall arrest distance [25];
- evaluation of the maximum forces acting on the work site elements to which the anchor lines are attached;
- analysis of both single-span and multi-span horizontal anchor lines;
- possibility of configuring parameters b_0, b_1, η, and k_1 to reflect the characteristics of different textile materials.

Given the differences between the numerical simulations and laboratory test results, further efforts should be made to improve the model by:
– taking into consideration the initial tension in the anchor line generated by the force of gravity and by human adjustment;
– taking into consideration anchor line deflection under its own weight;
– expanding the analysis to include other points of loading than the span midpoint;
– determining load-elongation characteristics for a wide range of textile ropes and webbing to enable their analysis;
– expanding the model to include energy-absorbing elements, such as textile shock-absorbers installed at points where the anchor line is attached to the work site or connected to the full body harness.

The accomplishment of these objectives would lead to better correspondence of numerical simulations with the actual mechanical phenomena and enable analysis of a larger range of fall protection equipment.

The present publication is based on the results of Phase III of the National Programme "Safety and working conditions improvement," funded in the years 2014-2016 in the area of tasks related to services for the State by the Ministry of Labour and Social Policy. The Programme coordinator is the Central Institute for Labour Protection–National Research Institute.

References

1. Baszczyński K. Construction, basic requirements and methods of testing horizontal anchor lines which allow emploees to move during work at height (Konstrukcja, podstawowe wymagania i metody badań urządzeń kotwiczących umożliwiających przemieszczanie się pracownika na stanowiskach pracy na wysokości). Occupational Safety. Science and Practice, Warsaw, 2/2016, p. 13-17.
2. Sulowski AC. Fall protection systems – selection of equipment. In A.C. Sulowski (Ed.), Fundamentals of fall protection (pp. 303-320). Toronto, Canada: International Society for Fall Protection 1991.
3. Baszczyński K, Zrobek Z. Horizontal anchor lines made of steel wire ropes (Stalowe poziome liny zaczepowe). Occupational Safety. Science and Practice, Warsaw, 6/1998, p. 18-21.
4. European Committee for Standardization (CEN). (2008). Personal fall protection equipment – Personal fall protection systems (Standard No. EN 363: 2008). Brussels, Belgium.
5. European Committee for Standardization (CEN). (2012). Personal fall protection equipment – Anchor devices (Standard No. EN 795: 2012). Brussels, Belgium.
6. European Committee for Standardization (CEN). (2012). Personal fall protection equipment – Anchor devices – Recommendations for anchor devices for use by more than one person simultaneously (Technical Specification No. 16415: 2013). Brussels, Belgium.
7. Directive 89/686/EEC – personal protective equipment
8. Miura N & Sulowski AC. Introduction to horizontal lifelines. In A.C. Sulowski (Ed.) (pp. 217-283) Fundamentals of fall protection. Toronto, Ont, Canada: International Society for Fall Protection, 1991.
9. Baszczyński K, Zrobek Z. Dynamic Performance of Horizontal Flexible Anchor Lines During Fall Arrest – A Numerical Method of Simulation. *International Journal of Occupational Safety and Ergonomics*, Central Institute for Labour Protection 2000l 6, 4: 521-534.
10. Baszczyński K, Jachowicz M. Load-Elongation Characteristics of Connecting and Shock-Absorbing Components of Personal Fall Arrest Systems. *Fibres and Textiles in Eastern Europe* 2012; 20, 6A(95): 78-85.

11. Baszczyński K. Modeling the performance of selected textile elements of personal protective equipment protecting against falls from a height during fall arrest. *Fibres and Textiles in Eastern Europe* 2013, 21, 4(100): 130-136.
12. Robinson L. Development of a technique to measure the dynamic loading of safety harness and lanyard webbing. HSL/2006/37.
13. Bedogni V, Manes A. A constitutive equation for the behavior of a mountaineering rope under stretching during a climber's fall. *Procedia Engineering* 2011; 10: 3353-3358.
14. Baszczyński K. Effect of Repeated Loading on Textile Rope and Webbing Characteristics in Personal Equipment Protecting Against Falls from a Height. *Fibres and Textiles in Eastern Europe* 2015; 23, 4(112): 110-118. DOI: 10.5604/12303666.1152741
15. Leech CM. The modelling of friction in polymer fibre ropes. Pergamon. *International Journal of Mechanical Sciences* 2002; 44: 621-643.
16. Bles G, Nowacki WK, Tourai A. Experimental study of the cyclic visco-elasto-plastic behaviour of a polyamide fibre strap. *International Journal of Solids and Structures* 2009; 46: 2693-2705.
17. Ghoreishi SR, Cartraud P, Davies P, Messager T. Analytical modeling of synthetic fiber ropes subjected to axial loads. Part I: A new continuum model for multilayered fibrous structures. *International Journal of Solids and Structures* 2007; 44, 9: 2924-2942.
18. Analytical modeling of synthetic fiber ropes. Part II: A linear elastic model for 1 + 6 fibrous structures. *International Journal of Solids and Structures* 2007; 44, 9: 2943-2960.
19. Aksan S. The effect of fatigue stretching frequency on the strength parameters of yarn In Polish. *Prace Instytutu Włókiennictwa*, Łódź 1987: p. 5-35.
20. Mainardi F, Spada G. Creep, relaxation and viscosity properties for basic fractional models in rheology. *The European Physical Journal, Special Topics* 2011; 193: 133-160.
21. Świtka R, Husiar B. Dyskretna analiza modeli reologicznych. *Journal of Theoretical and Applied Mechanics* 1984; 22: 1-2: p. 209-233.
22. Mathcad 2001 Professional, Warszawa 2003, ISBN 83-87674-56-7.
23. European Committee for Standardization (CEN). Personal protective equipment against falls from a height – Test methods (Standard No. EN 364:1992). Brussels, Belgium.
24. http://www.imagesystems.se/image-systems-motion-analysis/products/tema-motion.aspx
25. Sulowski AC. Fundamentals of fall protection. Residual risk in fall arresting systems. Toronto: International Society for Fall Protection 1991; 321-344.

Received 21.10.2016 Reviewed 28.04.2017